reactions

MDPI

Article

Theoretical Study of the Halogen Concentration Effect on the 1,3-Butadiene Polymerization Catalyzed by the Neodymium-Based Ziegler–Natta System

Alexey N. Masliy [1,*], Ildar G. Akhmetov [2], Andrey M. Kuznetsov [1] and Ilsiya M. Davletbaeva [3]

[1] Department of Inorganic Chemistry, Kazan National Research Technological University, Karl Marx Street 68, 420015 Kazan, Russia; am_kuznetsov@kstu.ru
[2] Nizhnekamsk Chemical and Technological Institute (Branch), Kazan National Research Technological University, Karl Marx Street 68, 420015 Kazan, Russia; akhmetovig@kstu.ru
[3] Technology of Synthetic Rubber Department, Kazan National Research Technological University, Karl Marx Street 68, 420015 Kazan, Russia; davletbaeva09@mail.ru
* Correspondence: masliy@kstu.ru

Abstract: In this work, an attempt is made to theoretically substantiate the experimentally known facts of the influence of halogen concentration on the catalytic properties of the neodymium-based Ziegler–Natta system. Based on the structural and thermochemical data obtained using modern methods of quantum chemistry, the process of the 1,3-butadiene *cis*-1,4-polymerization under the model active centers of the neodymium Ziegler–Natta catalysts with different contents of chloride ions was studied. Results are presented that explain the increase in the *cis*-stereospecificity and activity of the polymerization system with an increase in the content of the chloride ions in the neodymium catalytic system. Reasons were established for the decrease in the concentration of active centers relative to the introduced Nd(III) with an excess of chloride ions and the occurrence of the *anti-syn* isomerization as a source of the formation of the *trans*-1,4-structures in the *cis*-1,4-polybutadiene.

Keywords: DFT; ONIOM; 1,3-butadiene polymerization; stereospecificity; *cis*-1,4-polybutadiene; neodymium-based Ziegler–Natta catalyst

check for updates

Citation: Masliy, A.N.; Akhmetov, I.G.; Kuznetsov, A.M.; Davletbaeva, I.M. Theoretical Study of the Halogen Concentration Effect on the 1,3-Butadiene Polymerization Catalyzed by the Neodymium-Based Ziegler–Natta System. *Reactions* **2024**, *5*, 753–764. https://doi.org/10.3390/reactions5040037

Academic Editor: Mariusz Mitoraj

Received: 31 August 2024
Revised: 23 September 2024
Accepted: 3 October 2024
Published: 7 October 2024

Copyright: © 2024 by the authors. Licensee MDPI, Basel, Switzerland. This article is an open access article distributed under the terms and conditions of the Creative Commons Attribution (CC BY) license (https://creativecommons.org/licenses/by/4.0/).

1. Introduction

Ziegler–Natta catalysts, first used for the polymerization of α-olefins, are in demand and being studied in this capacity to this day [1–6]. At the same time, the creation of Ziegler–Natta catalysts laid the foundation for the industrial production of stereoregular synthetic rubbers [7,8]. Over the past three decades, technologies for the production of SR using lanthanide, primarily neodymium, ion-coordination-type catalysts have been actively developed [9–15]. Despite the large number of works, research in this area continues to be relevant. This is due to the unique capabilities of neodymium-containing catalytic systems, which include high activity, stereoregularity and controlled molecular parameters of the resulting polymers, and the ability to use various monomers in the synthesis [16–21]. This is due to the unique capabilities of the neodymium catalytic systems, such as their versatility, high activity, stereoregularity, and ability to regulate the molecular weight characteristics of the synthesized polydienes [22–24]. In industrial practice, for the production of synthetic rubbers, double [25–29] and triple [30–33] neodymium catalytic systems are used as a rule. Depending on the synthesis conditions and type of initial catalyst components, the properties of the catalytic system and, accordingly, the polymer formed during the polymerization process can be varied over a wide range.

Despite the diversity of the starting components of double and ternary lanthanide catalytic systems, researchers agree on similar models of the structure of active polymerization sites. In our opinion, Yu. B. Monakov's group has advanced most deeply in understanding

the structure of the neodymium catalytic systems for the polymerization of dienes [34–36]. They found that the neodymium-based Ziegler–Natta catalytic systems are polycentered and can contain up to six types of active centers in their structure. Depending on the synthesis conditions, the catalytic system contains a certain set of active centers. At the same time, one of the key parameters is the halogen content, primarily chlorine, in the Nd(III) coordination sphere. It was found that the maximum *cis*-1,4-stereospecificity of catalytically active centers corresponds to the structure with the highest chlorine content in the Nd(III) environment and decreases until inversion to *trans*-stereospecificity with a decrease in the chlorine content in the active center [37,38].

This work is the continuation of the research using modern methods of quantum chemistry, in which, based on structural and thermochemical data, a theoretical justification of the existing experimental data is carried out [39,40] with the aim of further creating new effective industrial neodymium-based Ziegler–Natta catalysts.

The data given in Table 1 [41–43] were used as experimental kinetic parameters of the polymerization process of 1,3-butadiene and the microstructure of the resulting polybutadiene obtained at various [Cl]:[Nd] molar ratios in the neodymium catalyst.

Table 1. Kinetic parameters of 1,3-butadiene polymerization and microstructure of polybutadiene obtained at different [Cl]:[Nd] molar ratios.

[Cl]:[Nd]	W_p, mol/(l min)	k_g, l/(mol min)	γ_{Nd}, %	*cis*-1,4-Content, %	*trans*-1,4-Content, %	1,2-Content, %
1.0	0.03	520	18	95.5	3.4	1.1
2.0	0.18–0.20	2900–2950	32–37	96.0–96.5	2.5–3.0	1.0
3.0	0.25–0.28	4800–4950	27–29	97.1	1.9	1.0
4.0	0.14–0.16	4800–5187	13–17	98.1	0.9	1.0

W_p—polymerization rate; k_g—growth rate constant; γ_{Nd}—the proportion of neodymium in active centers.

According to the data given in Table 1, in the studied range of [Cl]:[Nd] ratios, the catalytic system under consideration is *cis*-stereoregulatory. As the inner coordination sphere of Nd(III) becomes saturated with chlorine ions, the growth rate constant of the polymer chain monotonically increases. At the same time, the overall rate of the polymerization process changes extremely, reaching a maximum at the [Cl]:[Nd] ratio of 3, which is due to a change in the proportion of active sites (AS) relative to the introduced Nd(III). The microstructure of the polymer correlates with the chlorine content in the catalyst, an increase that leads to an increase in the content of *cis*-1,4 structures in the polymer. Experimental data indicate that each [Cl]:[Nd] ratio in the catalyst is characterized by its own set of active centers with a predominant content of centers of a certain type, which has its own kinetic parameters and forms a polymer with certain characteristics.

In accordance with an analysis of the literature data and experimental results [37–40], Figure 1 shows models of the active centers of the neodymium catalytic system in which the chlorine content changes. Previously, in [39], a detailed structural and thermochemical analysis of the active center model, AS(IV), was carried out, and the mechanism of its catalytic action was studied. The results of the study not only confirmed the efficiency of the model, but also made it possible to propose a refinement of the classical mechanism of *cis*-stereoregulation of a growing polymer chain.

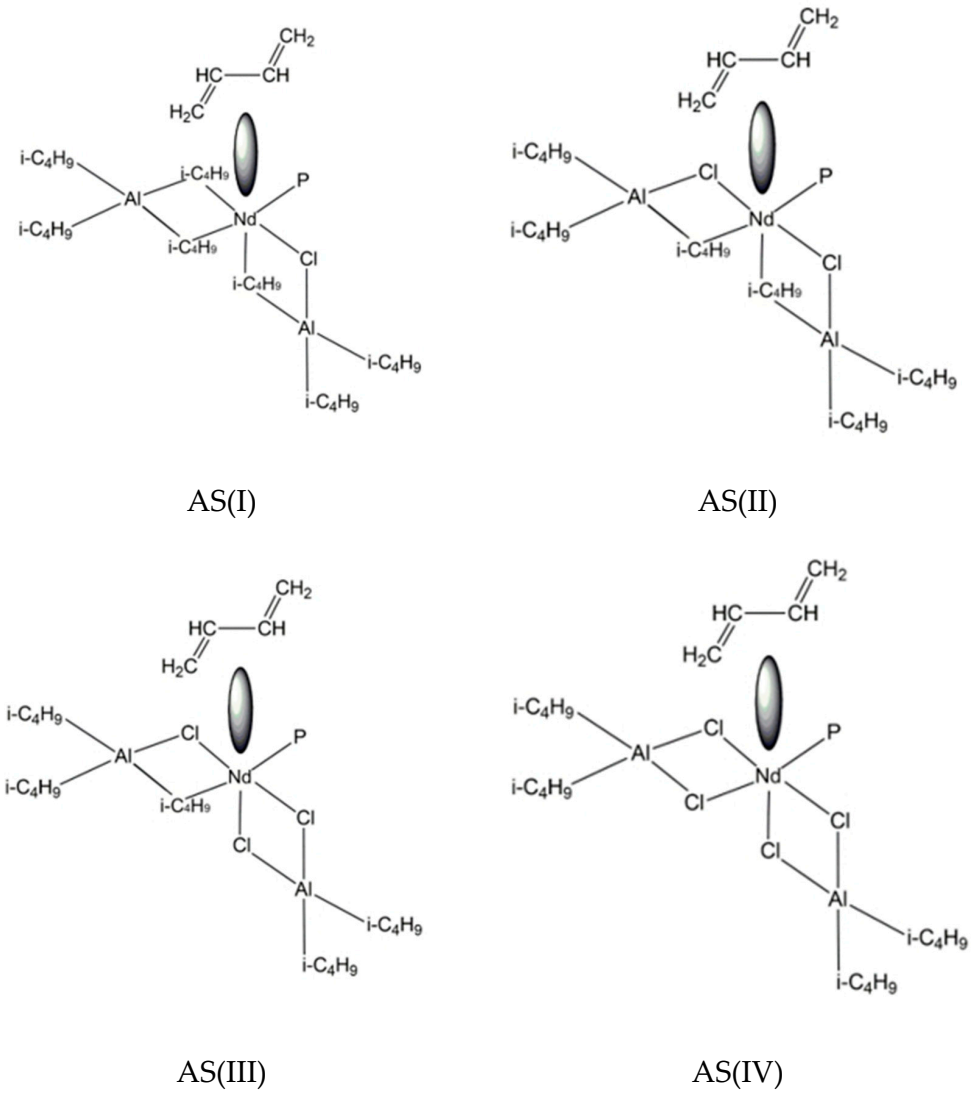

Figure 1. Models of the neodymium-based Ziegler–Natta catalytic systems active sites (AS). P—growing polymer chain/*i*-C_4H_9, AS(I), AS(II), AS(III), and AS(IV) — model active centers, containing 1, 2, 3, and 4 chlorine at-oms in the Nd(III) coordination sphere, respectively.

2. Computational Details

Since this work is a direct continuation of our previous studies [39,40], the same methods and approaches were used here.

Quantum-chemical calculations were carried out using the Orca 5.0.3 program package [44,45] in the framework of the ONIOM two-layer (QM1/QM2) model [46], in which a part is allocated in the system under study, calculated using the high-level quantum chemical method QM1, and the entire system as a whole is calculated using the low-level QM2 method. Then, the results of these two calculations are combined using a special technique. The hybrid density functional B3LYP [47,48] was used as a high-level method (QM1) in the calculations in combination with the second-generation split-valence triple-ζ atomic basis set def2-TZVP by Ahlrichs et al. [49,50]. The core electrons of the neodymium atom were described using the Def2-ECP pseudopotential [51] recommended for use with Def2 basis sets, which also takes into account scalar relativistic effects for this element. The tight-binding DFT (semi-empirical DFT) method XTB1 by Grimme et al. [52,53] was chosen as a low-level QM2 method. Since the Nd(III) ion has three unpaired electrons and the total multiplicity of all the complexes under study is 4 (confirmed by a series of additional calculations), the spin-unrestricted method was used for all calculations.

A feature of the systems under study is that weak Van der Waals interactions play an important role in them, and these were taken into account in the framework of the D3 semi-empirical model [54] by Grimme et. al.

All calculations were performed with full optimization of molecular geometry without any symmetry constraints. Since the polymer synthesis is carried out in hexane, geometry optimization was carried out taking into account the influence of the solvent (hexane) in the continuum model ALPB—a method of analytical linearization of the Poisson–Boltzmann equation [55].

The calculations of vibrational spectra performed after geometry optimization did not contain imaginary modes. This means that the structures found correspond to minima on the total potential energy surface. These calculations were also used to estimate the thermal corrections needed to calculate the total Gibbs free energy of particles (at 298.15 K and 1 atm).

To calculate the activation energies of the process, we used the standard procedure for searching for the transition state. The calculations of vibrational spectra performed after geometry optimization did not contain imaginary modes for minima and contained one imaginary mode for transition states. Each found transition state was checked for compliance with the considered chemical process using the internal reaction coordinate (IRC) procedure.

3. Results and Discussion

In this work, the process of cis-1,4-polymerization of 1,3-butadiene under the action of model active centers AS(I), AS(II), AS(III), and AS(IV) containing 1, 2, 3, and 4 chlorine atoms in the Nd(III) coordination sphere, respectively, was studied. The analysis of the structural characteristics and thermodynamic features of the formation of the AS(IV) complex with 1,3-butadiene, carried out in [39], and the calculation of changes in the activation energy and Gibbs free energy of the polymerization process in this system made it possible to quite reasonably assume the following stages of the formation of 1,4- polybutadiene. The first stage involves the coordination of η-*trans*-C_4H_6 on the active site; then, in the case of the formation of *cis*-1,4-polybutadiene in the region of the coordination interaction, *trans-cis* isomerization of *trans*-1,3-butadiene occurs, and, finally, the insertion of 1,3-butadiene into the reactive growing polymer chain takes place. Based on this, the main routes of the stages of initiation and growth of the polymer chain, taking into account the transition states for the systems under study during the formation of 1,4-polybutadiene, can be represented by the following schemes:

1. Initiation stage:

$$i\text{-}C_4H_9\text{-AS-T} \rightarrow i\text{-}C_4H_9\text{-AS-T(TS2)} \rightarrow i\text{-}C_4H_9\text{-T-AS} \quad (1)$$

$$i\text{-}C_4H_9\text{-AS-T} \rightarrow i\text{-}C_4H_9\text{-AS-TC(TS1)} \rightarrow i\text{-}C_4H_9\text{-AS-C} \rightarrow i\text{-}C_4H_9\text{-AS-C(TS2)} \rightarrow \rightarrow i\text{-}C_4H_9\text{-C-AS} \quad (2)$$

2. Growth stage (insertion of 1,3-butadiene into the reactive growing polymer chain):

$$i\text{-}C_4H_9\text{-P-AS-T} \rightarrow i\text{-}C_4H_9\text{-P-AS-T(TS2)} \rightarrow i\text{-}C_4H_9\text{-P-T-AS} \quad (3)$$

$$i\text{-}C_4H_9\text{-P-AS-T} \rightarrow i\text{-}C_4H_9\text{-P-AS-TC(TS1)} \rightarrow i\text{-}C_4H_9\text{-P-AS-C} \rightarrow i\text{-}C_4H_9\text{-P-AS-C(TS2)} \rightarrow \rightarrow i\text{-}C_4H_9\text{-P-C-AS} \quad (4)$$

where: AS is AS(I), AS(II), AS(III), or AS(IV); T is η-*trans*-C_4H_6 or π-*syn*-C_4H_6; C is η-*cis*-C_4H_6 or π-*anti*-C_4H_6; P is growing polymer chain; TS1 is transition state caused by the *trans-cis* transformation of 1,3-butadiene; and TS2 is transition state caused by the insertion of 1,3-butadiene into the reactive growing polymer chain.

Consider the initiation steps for AS(I), AS(II), AS(III), and AS(IV), where the calculated Gibbs free energies of reactions (1) and (2) are given in Table 2.

Table 2. Gibbs free energy and activation energy (kJ/mol) of the initiation stage for AS(I)-AS(IV).

Initial Structure	$\Delta G^{\neq}_{298}$ (*trans-cis*)	ΔG_{298} (*trans-cis*)	$\Delta G^{\neq}_{298}$ (Polymer)	$\Delta G^{\neq}_{298}$ (Total)	ΔG_{298} (Polymer)	Product
i-C_4H_9-AS(I)-T	41.4	10.4	64.9	75.3	−38.0	*i*-C_4H_9-C-AS(I)
i-C_4H_9-AS(I)-T			81.6	81.6	−70.3	*i*-C_4H_9-T-AS(I)
i-C_4H_9-AS(II)-T	43.9	12.8	56.8	69.6	−66.6	*i*-C_4H_9-C-AS(II)
i-C_4H_9-AS(II)-T			87.9	87.9	−54.8	*i*-C_4H_9-T-AS(II)
i-C_4H_9-AS(III)-T	41.1	11.4	59.2	70.6	−61.9	*i*-C_4H_9-C-AS(III)
i-C_4H_9-AS(III)-T			86.2	86.2	−51.5	*i*-C_4H_9-T-AS(III)
i-C_4H_9-AS(IV)-T	43.0	6.6	54.3	60.9	−51.7	*i*-C_4H_9-C-AS(IV)
i-C_4H_9-AS(IV)-T			67.0	67.0	−55.1	*i*-C_4H_9-T-AS(IV)

As can be seen from the data given in Table 2 for the AS(I), AS(II), and AS(III) complexes, the same trend is observed as for AS(IV); namely, that the total activation energy of the initiation stage by introducing 1.3-butadiene in the *cis*-form is lower than when forming the *i*-C_4H_9-T-AS structure. Among other features, it should be noted that the *trans-cis* isomerization of coordinately bound 1,3-butadiene on all active centers proceeds with approximately the same activation energy, ~41–44 kJ/mol, while the most favorable structure is characteristic of the active center with the maximum chlorine content.

The highest total activation energy for the process of the insertion of 1,3-butadiene into the reactive growing polymer chain, according to reaction (2), is observed for AS(I). At the same time, AS(II) and AS(III) have approximately the same total activation energy, which is 5 kJ/mol less in comparison with AS(I). AS(IV) has the lowest total activation energy, which is approximately 10 kJ/mol less than that of AS(II). Also, the highest total activation energy for the process of the insertion of 1,3-butadiene into the reactive growing polymer chain in the form of a *trans*-unit is observed for AS(II). For AS(III), this activation energy is lower by only 1.7 kJ/mol, and for AS(I), it is lower by another 5 kJ/mol. As in the case of reaction (2), for reaction (1), AS(IV) has the lowest activation energy, and this value is 14 kJ/mol lower than that of AS(I). As for the products of reactions (1) and (2), the following trend is observed here: for AS(IV), the *cis*- and *trans*-forms of the final polymer unit at the initiating stage have almost the same stability, with a slight (~3 kJ/mol) advantage of *trans*-forms. For AS(II) and AS(III), the situation is similar, but the *cis*-form of the terminal unit has greater stability with an advantage of ~10 kJ/mol. At the same time, for AS(I), the situation is fundamentally different; here, the *trans*-form of the terminal unit is approximately twice as advantageous as the *cis*-form. This is consistent with the increase in the proportion of active centers relative to the introduced neodymium at [Cl]:[Nd] in the range from 1.0 to 2.0, but does not correlate with a further decrease in the AS concentration with increasing chlorine content (Table 1). To explain this, the energy characteristics of model AS structures were additionally studied by calculating the thermodynamic parameters of the reactions of a gradual increase in the chlorine content in AS. Diisobutylaluminum chloride was used as a model source of chlorine (see reactions (5)–(9)):

$$i\text{-}C_4H_9\text{-AS(I)-T} + Al(C_4H_9)_2Cl \rightarrow i\text{-}C_4H_9\text{-AS(II)-T} + Al(C_4H_9)_3 \quad (5)$$

$$i\text{-}C_4H_9\text{-AS(II)-T} + Al(C_4H_9)_2Cl \rightarrow i\text{-}C_4H_9\text{-AS(III)-T} + Al(C_4H_9)_3 \quad (6)$$

$$i\text{-}C_4H_9\text{-AS(III)-T} + Al(C_4H_9)_2Cl \rightarrow i\text{-}C_4H_9\text{-AS(IV)-T} + Al(C_4H_9)_3 \quad (7)$$

$$i\text{-}C_4H_9\text{-AS(IV)-T} + Al(C_4H_9)_2Cl \rightarrow \text{Cl-AS(IV)-T} + Al(C_4H_9)_3 \quad (8)$$

$$i\text{-}C_4H_9\text{-AS(IV)-T} + Al(C_4H_9)_2Cl \rightarrow i\text{-}C_4H_9\text{-AS(IV)-Cl-}Al(C_4H_9)_2 + \textit{trans}\text{-}C_4H_9 \quad (9)$$

In this case, reactions (5)–(7) represent a step-by-step transition from AS (I) to AS(IV), and reactions (8) and (9) model the so-called "excess chlorination" of AS (IV) and represent the formation of complexes that are not active in the polymerization process (Figure 2).

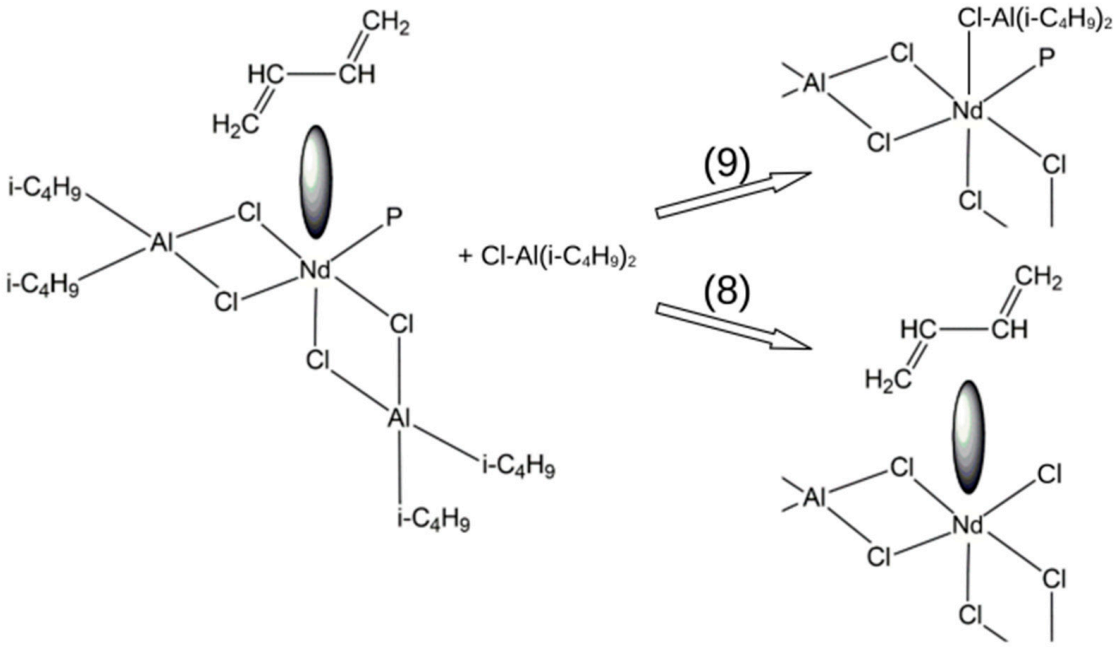

Figure 2. Models of structures formed by reactions (8) and (9). P—growing polymer chain/*i*-C_4H_9. A fragment of the AS is shown in the right part of the picture for clarity.

The obtained thermodynamic parameters of reactions (5)–(9) are given in Table 3. It can be seen that all reactions are exothermic and also have a negative change in Gibbs free energy (with the exception of reaction (9)); that is, they must proceed under standard conditions. Thus, structures with more chlorine content should be more stable. This is confirmed by an increase in the proportion of active centers during the transition from AS(I) to AS(II). However, a further increase in the chlorine content in the catalytic system and the transition from AS(II) to AS(III) and further to AS(IV) is accompanied by a decrease in the concentration of AS capable of reacting polymerization. Most likely, this is due to the formation of structures in which there is no possibility of the initiation stage occurring; namely, the formation of structures in which the chlorinating agent displaces the terminal isobutyl fragment in reaction (8) or replaces 1,3-butadiene in reaction (9). As can be seen from the data obtained, reaction (8) proceeds quite efficiently, and reaction (9) is theoretically possible. It should be noted that the change in entropy in reactions (5)–(7) has a positive value and suggests that, according to calculations, the process of transforming of active centers from the AS(I) to AS(IV) state is irreversible. In general, the results presented in Table 3 for the first time reasonably explain the decrease in catalyst activity during "excessive chlorination" and can be the subject of a separate study, which will consider not only AS(IV) but also other types of AS.

Table 3. Thermodynamic parameters of the reactions (5)–(9).

Reaction Parameter	Reaction No.				
	5	**6**	**7**	**8**	**9**
ΔH^0_{298}, kJ/mol	−33.5	−41.6	−89.1	−76.8	−8.4
ΔS^0_{298}, J/(mol·K)	18.1	13.3	15.6	−11.7	−33.6
ΔG^0_{298}, kJ/mol	−38.9	−47.5	−93.7	−73.3	1.5

Summing up the consideration of the stage of the 1,3-butadiene polymerization process initiation under the influence of the model structures of the active centers AS(I), AS(II), AS(III), and AS(IV), we can conclude that the introduction of the first 1,3-butadiene molecule is already characterized by the formation of the π-*anti*-C_4H_6-AS complex, as a future fragment of the *cis*-1,4-unit of the polymer chain. An increase in the molar ratio [Cl]:[Nd] from 1.0 to 4.0 in the AS structure is accompanied by a decrease in the Gibbs energy of the resulting structures and a decrease in the total activation energy of the initiation stage; that is, an increase in its efficiency. At the same time, the observed decrease in the proportion of active centers relative to the introduced Nd(III) at the [Cl]:[Nd] ratio of 3.0 and 4.0 is explained by the formation of structures that are inactive during the polymerization process.

Next, we considered the stage of polymer chain growth. Since it was previously shown that the stabilization of the calculated values of the energy parameters of the system occurs after the formation of the Kuhn segment, which is a polymer fragment of the three monomer units, it was decided to proceed directly to this stage. AS(IV) structures obtained in [39] were used as a model for the starting compounds. In order not to consider all possible complexes, it was decided to study only the process of adding 1,3-butadiene to the *i*-C_4H_9-CC-AS and *i*-C_4H_9-CT-AS complexes. Additionally, for all AS, the formation of the *i*-C_4H_9-CCCC-AS structure was considered. The results obtained are presented in Table 4.

Table 4. Gibbs free energy and activation energy (kJ/mol) of the polymer chain growth stage for AS(I)-AS(IV).

Initial Structure	$\Delta G^{\neq}_{298}$ (*trans-cis*)	ΔG_{298} (*trans-cis*)	$\Delta G^{\neq}_{298}$ (Polymer)	$\Delta G^{\neq}_{298}$ (Total)	ΔG_{298} (Polymer)	Product
i-C_4H_9-CC-AS(I)-T	29.5	23.5	63.9	87.4	−15.0	*i*-C_4H_9-CCC-AS(I)
i-C_4H_9-CCC-AS(I)-T	28.9	23.3	64.0	87.3	−35.1	*i*-C_4H_9-CCCC-AS(I)
i-C_4H_9-CC-AS(I)-T			102.8	102.8	−58.7	*i*-C_4H_9-CCT-AS(I)
i-C_4H_9-CT-AS(I)-T	32.1	22.5	60.8	82.3	−18.4	*i*-C_4H_9-CTC-AS(I)
i-C_4H_9-CT-AS(I)-T			90.9	90.9	−56.6	*i*-C_4H_9-CTT-AS(I)
i-C_4H_9-CC-AS(II)-T	35.5	7.3	65.0	72.3	−21.3	*i*-C_4H_9-CCC-AS(II)
i-C_4H_9-CCC-AS(II)-T	34.0	7.6	63.7	71.3	−50.3	*i*-C_4H_9-CCCC-AS(II)
i-C_4H_9-CC-AS(II)-T			95.7	95.7	−53.7	*i*-C_4H_9-CCT-AS(II)
i-C_4H_9-CT-AS(II)-T	23.2	17.6	60.4	78.0	−29.0	*i*-C_4H_9-CTC-AS(II)
i-C_4H_9-CT-AS(II)-T			94.5	94.5	−2.2	*i*-C_4H_9-CTT-AS(II)
i-C_4H_9-CC-AS(III)-T	29.9	14.8	51.5	66.8	−27.3	*i*-C_4H_9-CCC-AS(III)
i-C_4H_9-CCC-AS(III)-T	29.5	7.6	51.8	59.4	−35.7	*i*-C_4H_9-CCCC-AS(III)
i-C_4H_9-CC-AS(III)-T			104.0	104.0	−51.7	*i*-C_4H_9-CCT-AS(III)
i-C_4H_9-CT-AS(III)-T	32.1	26.2	56.0	82.2	−2.8	*i*-C_4H_9-CTC-AS(III)
i-C_4H_9-CT-AS(III)-T			99.2	99.2	−25.3	*i*-C_4H_9-CTT-AS(III)
i-C_4H_9-CC-AS(IV)-T	24.6	14.6	51.7	66.3	−35.0	*i*-C_4H_9-CCC-AS(IV)
i-C_4H_9-CCC-AS(IV)-T	24.7	6.3	54.2	60.5	−60.4	*i*-C_4H_9-CCCC-AS(IV)
i-C_4H_9-CC-AS(IV)-T			102.0	102.0	−52.9	*i*-C_4H_9-CCT-AS(IV)
i-C_4H_9-CT-AS(IV)-T	21.4	12.9	70.1	83.0	−8.9	*i*-C_4H_9-CTC-AS(IV)
i-C_4H_9-CT-AS(IV)-T			77.5	77.5	−40.3	*i*-C_4H_9-CTT-AS(IV)

The analysis of the data presented in Table 4 can begin with a statement of the fact that, for all model structures of active centers, the insertion of *trans*-1,3-butadiene into the reactive growing polymer chain occurs with a higher activation energy in comparison

with the insertion of *cis*-1,3-butadiene, which occurs in two stages. When considering the *cis*-1,4-polybutadiene reaction formation in the series AS(I), AS(II), AS(III), and AS(IV), a consistent decrease in the total activation energy is observed. However, for AS(I) and AS(II), the total activation energy value is almost the same. In almost all cases, the growing polybutadiene chain with a terminal *trans*-unit turns out to be thermodynamically more stable than the growing polybutadiene chain with a terminal *cis*-unit. This indicates that when the rate of polymerization of 1.3-butadiene decreases, *anti-syn* isomerization of the terminal unit becomes possible. The results obtained are in good agreement with the experimental data of Table 1; namely, an increase in the rate constant of the polymerization reaction and the content of *cis*-1,4-units in the polymer upon transition from AS(I) to AS(IV).

As noted above, all considered model active centers are *cis*-stereoregulatory. At the same time, the content of *trans*-1,4-units in polybutadiene can exceed 4.0% (Table 1). At the same time, for the physical and mechanical characteristics of the polymer, it is important how the "impurity" *trans*-1,4-units are distributed. A comparison of the total activation energies of reactions (3) and (4) shows that the bonding of the *cis*-1,3-butadiene to the terminal *cis*-unit of the growing polybutadiene chain occurs with a lower activation energy than the insertion to the terminal *trans*-unit for all types of active centers studied. For AS(IV), these activation energies are close, but the bonding of the *cis*-1,3-butadiene to the terminal *trans*-unit of the growing polybutadiene chain is somewhat more favorable. For reaction (4) of the insertion of the *cis*-1,3-butadiene to the terminal *trans*-unit of the reactive growing polybutadiene chain, the total activation energy is almost the same for all active centers and is ~82 kJ/mol. This allows us to conclude that the appearance of a terminal *trans*-unit in the growing polybutadiene chain in the case of AS(I), AS(II), and AS(III) should not lead to the appearance of the dyads of the *trans*-units. However, for AS(IV), the results obtained do not exclude the formation of small blocks of the *trans*-1,4 units.

It is also clear from the results in Table 4 that the total activation energies for the binding of 3 and 4 units to the polymer chain differ very slightly and are stabilized for each type of center at its own level. Thus, for AS(I), AS(II), AS(III), and AS(IV), these are ~87, ~71, ~60, and ~61 kJ/mol, respectively.

Next, we will analyze the most characteristic, from our point of view, bond lengths between the Nd(III) ion and 1,3-butadiene, as well as between the Nd(III) ion and the terminal π-allylic units of the growing polymer chain for AS(I)-AS (IV) (Table 5). For convenience of presentation and discussion of materials, we will accept the following notations: C^1, C^2, C^3, and C^4 are the carbon atoms of coordinately bound 1,3-butadiene, and C^α, C^β, C^γ, and C^δ are the carbon atoms of the terminal link of the growing polymer chain, where C^1 and C^α are the carbon atoms closest to the lanthanide. The analysis of the geometry of the initial complexes *i*-C_4H_9-AS+η-*trans*-C_4H_6, characteristic of the initiation stage, did not reveal fundamental differences in the molecular parameters for catalytic complexes with different chlorine contents. From Table 5, it follows that for all types of AS, the distance between Nd(III) and carbon atoms in the 1,3-butadiene in the *trans*-form is ~3 Å. This indicates that the main role in the binding of Nd(III) to the 1,3-butadiene is played by π-bonds, as well as electrostatic (dispersion and van der Waals) interactions.

For the chain growth stage, the geometry of the structures formed during the coordination of free 1,3-butadiene from the bulk of the reaction mixture to the *i*-C_4H_9-CCC-AS complex was calculated. Table 5 shows the structural characteristics for the complexes *i*-C_4H_9-CCC-AS(Mt)+η-*trans*-C_4H_6. It should be noted that, in this case, the monomer is characterized by η-4-*trans* coordination in Nd(III), and the terminal link of the growing polymer chain is in the π-*anti*-configuration. The observed distances between Nd(III) and the carbon atoms of the monomer and the growing polymer chain for AS(I), AS(II), AS(III), and AS(IV) are close; i.e., do not depend on the chlorine content in AS.

Thus, the presented results allow us to conclude that for the considered model active centers AS(I), AS(II), AS(III) and AS(IV), the key point that determines the cis-stereospecificity of the polymerization of 1,3-butadiene is the energy route of this process (Figure 3).

Table 5. Characteristic distances between Nd(III), 1,3-butadiene, and the growing polymer chain for the complexes *i*-C_4H_9-AS + η-*trans*-C_4H_6 и *i*-C_4H_9-CCC-AS + η-*trans*-C_4H_6.

Characteristic Distances, (R, Å)	AS (I)	AS (II)	AS (III)	AS (IV)
i-C_4H_9-AS + η-*trans*-C_4H_6 *				
R(Nd-C(i-C_4H_9))	2.431	2.387	2.377	2.414
R(Nd-C^1(C_4H_6))	3.504	3.244	3.261	3.513
R(Nd-C^2(C_4H_6))	3.148	3.021	3.048	3.161
R(Nd-C^3(C_4H_6))	3.19	3.143	3.151	3.111
R(Nd-C^4(C_4H_6))	3.559	3.605	3.616	3.415
R(C^1(C_4H_6)-C(i-C_4H_9)	3.634	3.476	3.46	3.571
i-C_4H_9-CCC-AS + η-*trans*-C_4H_6 **				
R(Nd-C^1(C_4H_6))	3.295	3.38	3.309	3.161
R(Nd-C^2(C_4H_6))	3.552	3.469	3.364	3.32
R(Nd-C^3(C_4H_6))	4.31	4.19	4.014	4.147
R(Nd-C^4(C_4H_6))	5.144	4.945	4.739	4.908
R(Nd-C^α(C_4H_6))	2.617	2.628	2.659	2.609
R(Nd-C^β(C_4H_6))	2.702	2.69	2.682	2.67
R(Nd-C^γ(C_4H_6))	2.732	2.751	2.672	2.758
R(Nd-C^δ(C_4H_6))	3.077	3.186	3.052	3.349
R(C^1(C_4H_6)-C^α(C_4H_6)	3.302	3.324	3.427	3.359

* Full optimized structures (Cartesian coordinates of atoms) are in the Supplementary Materials, Table S1. ** Full optimized structures (Cartesian coordinates of atoms) are in the Supplementary Materials, Table S2.

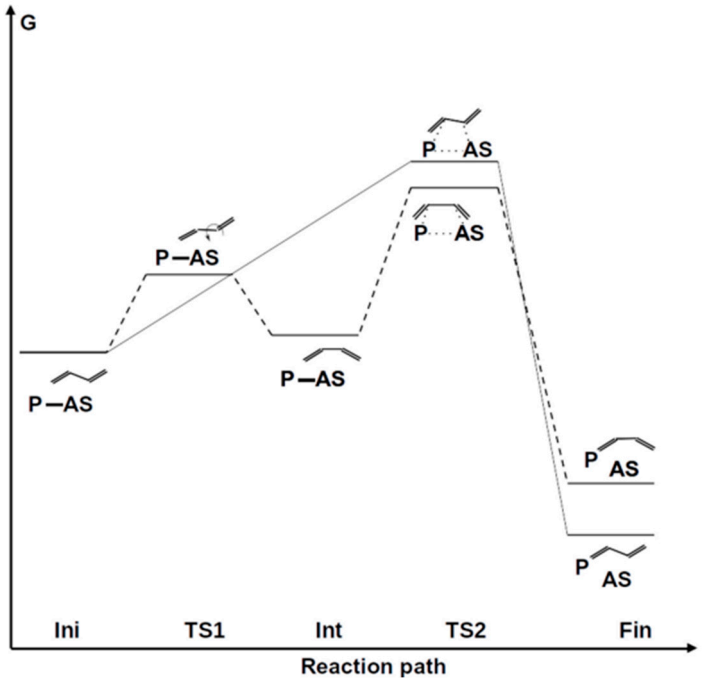

Figure 3. Energy diagram of the formation of 1,4-polybutadiene on AS, where P is *i*-C_4H_9 or the terminal π-allylic units of the growing polymer chain, TS1 is the transition state due to the *trans-cis* transformation of 1,3-butadiene, Int is the intermediate of the *cis*-1,3-butadiene interacting with AS, and TS2 is a transition state caused by the incorporation 1,3-butadiene into the polymer chain.

4. Conclusions

Using previously obtained experimental data, theoretical modeling of the stereoregular polymerization of 1,3-butadiene catalyzed by the model active centers with different chlorine contents in the neodymium-based Ziegler–Natta system was carried out. As a result, previously unknown peculiarities of the catalysis mechanism were obtained and

substantiated. Thus, it was shown that structures with a high content of chlorine in a neodymium catalytic system should be more stable and active. The decrease in the concentration of active centers relative to the introduced Nd(III) at a [Cl]:[Nd] ratio of 3.0 or more is explained by the formation of structures inactive during the polymerization process, in which there is no possibility of the insertion of 1,3-butadiene into the reactive growing polymer chain.

For all considered model active centers during the 1,3-butadiene polymerization, the bonding of *trans*-1,3-butadiene to the reactive growing polymer chain occurs with a higher activation energy in comparison with the insertion of *cis*-1,3-butadiene. In this case, an increase in the [Cl]:[Nd] ratio is accompanied by a decrease in the activation barrier, which is consistent with an increase in the chain propagation rate constant and the content of *cis*-1,4 structures in the resulting polybutadiene. The higher thermodynamic stability of the terminal unit of the growing polymer chain in the *trans*-configuration confirms the possibility of the *anti-syn* isomerization process as a source of the formation of *trans*-1,4 structures in the polybutadiene during slow polymerization.

An important result is the analysis of the geometry of the complexes at the stages of initiation and growth of the polymer chain, where it was established that the reason for the difference in the activity of the complexes and their *cis*-stereospecificity is not the steric factor, but the energy route of the polymerization process.

Supplementary Materials: The following supporting information can be downloaded at: https://www.mdpi.com/article/10.3390/reactions5040037/s1. Table S1: Atomic Cartesian coordinates (in Å) for optimized structures of *i*-C_4H_9-AS+η-*trans*-C_4H_6. Table S2: Atomic Cartesian coordinates (in Å) for optimized structures of i-C_4H_9-AS+η-*trans*-C_4H_6.

Author Contributions: Conceptualization, I.G.A. and I.M.D.; methodology, A.N.M. and A.M.K.; software, A.N.M.; validation, A.N.M., I.G.A., A.M.K., and I.M.D.; formal analysis, A.N.M. and I.G.A.; investigation, A.N.M. and I.G.A.; resources, A.M.K.; data curation, A.N.M. and I.G.A.; writing—original draft preparation, A.N.M. and I.G.A.; writing—review and editing, A.M.K. and I.M.D.; visualization, A.N.M.; supervision, I.M.D.; project administration, I.G.A. and I.M.D. All authors have read and agreed to the published version of the manuscript.

Funding: This work was carried out within the framework of the current scientific research plan of the University and is not supported by third-party funds.

Institutional Review Board Statement: Not applicable.

Informed Consent Statement: Informed consent was obtained from all subjects involved in the study.

Data Availability Statement: The data presented in this study are available on request from the corresponding author.

Conflicts of Interest: The authors declare no conflicts of interest.

References

1. D'amore, M.; Takasao, G.; Chikuma, H.; Wada, T.; Taniike, T.; Pascale, F.; Ferrari, A.M. Spectroscopic fingerprints of $MgCl_2/TiCl_4$ nanoclusters determined by machine learning and DFT. *J. Phys. Chem. C* **2021**, *125*, 20048–20058. [CrossRef]
2. Piovano, A.; Zarupski, J.; Groppo, E. Disclosing the Interaction between Carbon Monoxide and Alkylated Ti^{3+} Species: A Direct Insight into Ziegler–Natta Catalysis. *J. Phys. Chem. Lett.* **2020**, *11*, 5632–5637. [CrossRef] [PubMed]
3. Mehdizadeh, M.; Karkhaneh, F.; Nekoomanesh, M.; Sadjadi, S.; Emami, M.; Teimoury, H.; Posada-Pérez, S. Influence of the ethanol content of adduct on the Comonomer incorporation of related Ziegler–Natta catalysts in propylene (Co) polymerizations. *Polymers* **2023**, *15*, 4476. [CrossRef] [PubMed]
4. Pernusch, D.C.; Spiegel, G.; Paulik, C.; Hofer, W. Influence of Poisons Originating from Chemically Recycled Plastic Waste on the Performance of Ziegler–Natta Catalysts. *Macromol. React. Eng.* **2022**, *16*, 2100020. [CrossRef]
5. Hernández-Fernández, J.; Ortega-Toro, R.; Castro-Suarez, J.R. Theoretical–experimental study of the action of trace amounts of formaldehyde, propionaldehyde, and butyraldehyde as inhibitors of the ziegler–natta catalyst and the synthesis of an ethylene–propylene copolymer. *Polymers* **2023**, *15*, 1098. [CrossRef]
6. Blaakmeer, E.S.; Wensink, F.J.; van Eck, E.R.; de Wijs, G.A.; Kentgens, A.P. Preactive site in Ziegler–Natta catalysts. *J. Phys. Chem. C* **2019**, *123*, 14490–14500. [CrossRef]

7. Cooper, W.; Vaughan, G. Recent developments in the polymerization of conjugated dienes. *Prog. Polym. Sci.* **1967**, *1*, 91–160. [CrossRef]
8. Saltman, W.M. *The Stereo Rubbers*; Wiley-Interscience: New York, NY, USA, 1977; p. 897. [CrossRef]
9. Hsieh, H.L.; Yeh, H.C. Polymerization of butadiene and isoprene with lanthanide catalysts; characterization and properties of homopolymers and copolymers. *Rubber Chem. Technol.* **1985**, *58*, 117–145. [CrossRef]
10. Marina, N.G.; Monakov, Y.B.; Sabirov, Z.M.; Tolstikov, G.A. Lanthanide compounds—Catalysts of stereospecific polymerization of diene monomers. *Rev. Polym. Sci. USSR* **1991**, *33*, 387–417. [CrossRef]
11. Friebe, L.; Nuyken, O.; Obrecht, W. Neodymium-based Ziegler/Natta catalysts and their application in diene polymerization. In *Neodymium Based Ziegler Catalysts–Fundamental Chemistry*; Springer: Berlin/Heidelberg, Germany, 2006; pp. 1–154. [CrossRef]
12. Fischbach, A.; Anwander, R. *Neodymium Based Ziegler Catalysts Fundamental Chemistry*; Nuyken, O., Ed.; Springer: Berlin/Heidelberg, Germany, 2006; Volume 204, pp. 155–281. [CrossRef]
13. Zhang, Z.; Cui, D.; Wang, B.; Liu, B.; Yang, Y. Polymerization of 1, 3-conjugated dienes with rare-earth metal precursors. In *Molecular Catalysis of Rare-Earth Elements. Structure and Bonding*; Springer: Berlin/Heidelberg, Germany, 2010; pp. 49–108. [CrossRef]
14. Wang, F.; Liu, H.; Hu, Y.; Zhang, X. Lanthanide complexes mediated coordinative chain transfer polymerization of conjugated dienes. *Sci. China Technol. Sci.* **2018**, *61*, 1286–1294. [CrossRef]
15. Göttker-Schnetmann, I.; Kenyon, P.; Mecking, S. Coordinative Chain Transfer Polymerization of Butadiene with Functionalized Aluminum Reagents. *Angew. Chem.* **2019**, *131*, 17941–17945. [CrossRef]
16. González-Zapata, J.L.; Enríquez-Medrano, F.J.; González HR, L.; Revilla-Vázquez, J.; Carrizales, R.M.; Georgouvelas, D.; de León Gómez RE, D. Introducing random bio-terpene segments to high cis-polybutadiene: Making elastomeric materials more sustainable. *RSC Adv.* **2020**, *10*, 44096–44102. [CrossRef] [PubMed]
17. Cavalcante de Sá, M.C.; Córdova, A.M.T.; Díaz de León Gómez, R.E.; Pinto, J.C. Modeling of Isoprene Solution Coordinative Chain Transfer Polymerization. *Macromol. React. Eng.* **2021**, *15*, 2100005. [CrossRef]
18. Córdova, T.; Enríquez-Medrano, F.J.; Cartagena, E.M.; Villanueva, A.B.; Valencia, L.; Álvarez EN, C.; Díaz-de-León, R. Coordinative Chain Transfer Polymerization of Sustainable Terpene Monomers Using a Neodymium-Based Catalyst System. *Polymers* **2022**, *14*, 2907. [CrossRef]
19. Tereshchenko, K.A.; Ulitin, N.V.; Bedrina, P.S.; Shiyan, D.A.; Lifanov, A.D.; Madzhidov, T.I.; Volfson, S.I. Analysis of the Mechanism of Polybutadiene Synthesis in the Presence of the Neodymium Versatate+ Diisobutylaluminum Hydride+ Ethylaluminum Sesquichloride Catalytic System within the Solution of the Inverse Kinetic Problem. *Ind. Eng. Chem. Res.* **2022**, *61*, 15961–15969. [CrossRef]
20. Romano, E.; Budzelaar, P.H.; De Rosa, C.; Talarico, G. Unconventional Stereoerror Formation Mechanisms in Nonmetallocene Propene Polymerization Systems Revealed by DFT Calculations. *J. Phys. Chem. A* **2022**, *126*, 6203–6209. [CrossRef]
21. Quirk, R.P.; Kells, A.M.; Yunlu, K.; Cuif, J.P. Butadiene polymerization using neodymium versatate-based catalysts: Catalyst optimization and effects of water and excess versatic acid. *Polymer* **2000**, *41*, 5903–5908. [CrossRef]
22. Kwag, G. A highly reactive and monomeric neodymium catalyst. *Macromolecules* **2002**, *35*, 4875–4879. [CrossRef]
23. Zheng, W.; Yang, Q.; Dong, J.; Wang, F.; Luo, F.; Liu, H.; Zhang, X. Neodymium-based one-precatalyst/dual-cocatalyst system for chain shuttling polymerization to access cis-1, 4/trans-1, 4 multiblock polybutadienes. *Mater. Today Commun.* **2021**, *27*, 102453. [CrossRef]
24. Wang, H.; Cue JM, O.; Calubaquib, E.L.; Kularatne, R.N.; Taslimy, S.; Miller, J.T.; Stefan, M.C. Neodymium catalysts for polymerization of dienes, vinyl monomers, and ε-caprolactone. *Polym. Chem.* **2021**, *12*, 6790–6823. [CrossRef]
25. Iovu, H.; Hubca, G.; Simionescu, E.; Badea, E.G.; Dimonie, M. Polymerization of butadiene and isoprene with the NdCl3· 3TBP-TIBA catalyst system. *Die Angew. Makromol. Chem. Appl. Macromol. Chem. Phys.* **1997**, *249*, 59–77. [CrossRef]
26. Srinivasa Rao, G.S.; Upadhyay, V.K.; Jain, R.C. Polymerization of 1, 3-butadiene using neodymium chloride tripentanolate–triethyl aluminum catalyst systems. *J. Appl. Polym. Sci.* **1999**, *71*, 595–602. [CrossRef]
27. Ren, C.; Li, G.; Dong, W.; Jiang, L.; Zhang, X.; Wang, F. Soluble neodymium chloride 2-ethylhexanol complex as a highly active catalyst for controlled isoprene polymerization. *Polymer* **2007**, *48*, 2470–2474. [CrossRef]
28. Hu, Y.; Zhang, C.; Liu, X.; Gao, K.; Cao, Y.; Zhang, C.; Zhang, X. Methylaluminoxane-activated neodymium chloride tributylphosphate catalyst for isoprene polymerization. *J. Appl. Polym. Sci.* **2014**, *131*, 40153. [CrossRef]
29. Kularatne, R.N.; Yang, A.; Nguyen, H.Q.; McCandless, G.T.; Stefan, M.C. Neodymium catalyst for the polymerization of dienes and polar vinyl monomers. *Macromol. Rapid Commun.* **2017**, *38*, 1700427. [CrossRef]
30. Oehme, A.; Gebauer, U.; Gehrke, K.; Beyer, P.; Hartmann, B.; Lechner, M.D. The influence of the catalyst preparation on the homo-and copolymerization of butadiene and isoprene. *Macromol. Chem. Phys.* **1994**, *195*, 3773–3781. [CrossRef]
31. Boisson, C.; Barbotin, F.; Spitz, R. Polymerization of butadiene with a new catalyst based on a neodymium amide precursor. *Macromol. Chem. Phys.* **1999**, *200*, 1163–1166. [CrossRef]
32. Friebe, L.; Nuyken, O.; Windisch, H.; Obrecht, W. Polymerization of 1, 3-Butadiene Initiated by Neodymium Versatate/Diisobutylaluminium Hydride/Ethylaluminium Sesquichloride: Kinetics and Conclusions About the Reaction Mechanism. *Macromol. Chem. Phys.* **2002**, *203*, 1055–1064. [CrossRef]
33. Quirk, R.P.; Kells, A.M. Polymerization of butadiene using neodymium versatate-based catalyst systems: Preformed catalysts with SiCl4 as halide source. *Polym. Int.* **2000**, *49*, 751–756. [CrossRef]

34. Sigaeva, N.N.; Usmanov, T.S.; Budtov, V.P.; Monakov, Y.B. Effect of organoaluminum compound on kinetic nonuniformity and structure of active centers of neodymium catalytic systems in butadiene polymerization. *Russ. J. Appl. Chem.* **2001**, *74*, 1141–1146. [CrossRef]
35. Monakov, Y.B.; Sabirov, Z.M.; Urazbaev, V.N.; Efimov, V.P. Relationship between the stereospecificity of lanthanide catalysts and the structures of active sites and dienes, the nature of a cocatalyst, and preparation conditions. *Kinet. Catal.* **2001**, *42*, 310–316. [CrossRef]
36. Sigaeva, N.N.; Usmanov, T.S.; Budtov, V.P.; Spivak, S.I.; Zaikov, G.E.; Monakov, Y.B. The influence of the nature of organoaluminum compound on kinetic heterogeneity of active sites in lanthanide-based diene polymerization. *J. Appl. Polym. Sci.* **2003**, *87*, 358–368. [CrossRef]
37. Monakov, Y.B.; Sabirov, Z.M.; Urazbaev, V.N.; Efimov, V.P. Diene polymerization initiated by NdCl3. 3TBP-based catalytic systems. Multiplicity of active centers and their structure and stereospecificity distributions. *Polym. Science. Ser. A* **2002**, *44*, 228–231.
38. Urazbaev, V.N.; Efimov, V.P.; Sabirov, Z.M.; Monakov, Y.B. Structure of active centers, their stereospecificity distribution, and multiplicity in diene polymerization initiated by $NdCl_3$-based catalytic systems. *J. Appl. Polym. Sci.* **2003**, *89*, 601–603. [CrossRef]
39. Masliy, A.N.; Akhmetov, I.G.; Kuznetsov, A.M.; Davletbaeva, I.M. DFT and ONIOM Simulation of 1, 3-Butadiene Polymerization Catalyzed by Neodymium-Based Ziegler–Natta System. *Polymers* **2023**, *15*, 1166. [CrossRef]
40. Masliy, A.N.; Akhmetov, I.G.; Kuznetsov, A.M.; Davletbaeva, I.M. Comparative ONIOM modeling of 1, 3-butadiene polymerization using Nd (III) and Gd (III) Ziegler–Natta catalyst systems. *Int. J. Quantum Chem.* **2024**, *124*, e27297. [CrossRef]
41. Akhmetov, I.G.; Kozlov, V.G.; Salakhov, I.I.; Sakhabutdinov, A.G.; D'yakonov, G.S. Polymerisation kinetics and molecular characteristics of "neodymium" polybutadiene: Influence of halogenating agent concentration. *Int. Polym. Sci. Technol.* **2010**, *37*, 1–5. [CrossRef]
42. Salakhov, I.I.; Akhmetov, I.G.; Kozlov, V.G. Polymerization of butadiene during the action of the catalytic system neodymium versatate-diisobutylaluminum hydride-hexachloro-p-xylene. *Polym. Sci. Ser. B* **2011**, *53*, 385–390. [CrossRef]
43. Akhmetov, I.G. *Synthesis of Diene Rubbers Using Modified Catalytic Systems Based on Neodymium and Lithium Compounds. Dr. Chem. Sci. Diss.*; KNRTU Publisher: Kazan, Russia, 2013; 379p. (In Russian)
44. Neese, F. The ORCA Program System. *Wiley Interdiscip. Rev. Comput. Mol. Sci.* **2012**, *2*, 73–78. [CrossRef]
45. Neese, F. Software Update: The ORCA Program System, Version 4.0. *Wiley Interdiscip. Rev. Comput. Mol. Sci.* **2017**, *8*, 73–78. [CrossRef]
46. Dapprich, S.; Komáromi, I.; Byun, K.S.; Morokuma, K.; Frisch, M.J. A new ONIOM implementation in Gaussian98. Part I. The calculation of energies, gradients, vibrational frequencies and electric field derivatives. *J. Mol. Struct. THEOCHEM* **1999**, *461*, 1–21. [CrossRef]
47. Becke, A. Density-functional thermochemistry. III. The role of exact exchange. *J. Chem. Phys* **1993**, *98*, 5648. [CrossRef]
48. Lee, C.; Yang, W.; Parr, R.G. Development of the Colle-Salvetti correlation-energy formula into a functional of the electron density. *Phys. Rev. B* **1988**, *37*, 785. [CrossRef] [PubMed]
49. Weigend, F.; Ahlrichs, R. Balanced basis sets of split valence, triple zeta valence and quadruple zeta valence quality for H to Rn: Design and assessment of accuracy. *Phys. Chem. Chem. Phys.* **2005**, *7*, 3297–3305. [CrossRef]
50. Stoychev, G.L.; Auer, A.A.; Neese, F. Automatic generation of auxiliary basis sets. *J. Chem. Theory Comput.* **2017**, *13*, 554–562. [CrossRef]
51. Dolg, M.; Stoll, H.; Preuss, H. Energy-adjusted abinitio pseudopotentials for the rare earth elements. *J. Chem. Phys.* **1989**, *90*, 1730–1734. [CrossRef]
52. Grimme, S.; Bannwarth, C.; Shushkov, P. A robust and accurate tight-binding quantum chemical method for structures, vibrational frequencies, and noncovalent interactions of large molecular systems parametrized for all spd-block elements (Z = 1–86). *J. Chem. Theory Comput.* **2017**, *13*, 1989–2009. [CrossRef]
53. Bannwarth, C.; Ehlert, S.; Grimme, S. GFN2-xTB—An accurate and broadly parametrized self-consistent tight-binding quantum chemical method with multipole electrostatics and density-dependent dispersion contributions. *J. Chem. Theory Comput.* **2019**, *15*, 1652–1671. [CrossRef]
54. Grimme, S.; Antony, J.; Ehrlich, S.; Krieg, H. A consistent and accurate ab initio parametrization of density functional dispersion correction (DFT-D) for the 94 elements H-Pu. *J. Chem. Phys.* **2010**, *132*, 154104. [CrossRef]
55. Ehlert, S.; Stahn, M.; Spicher, S.; Grimme, S. Robust and efficient implicit solvation model for fast semiempirical methods. *J. Chem. Theory Comput.* **2021**, *17*, 4250–4261. [CrossRef]

Disclaimer/Publisher's Note: The statements, opinions and data contained in all publications are solely those of the individual author(s) and contributor(s) and not of MDPI and/or the editor(s). MDPI and/or the editor(s) disclaim responsibility for any injury to people or property resulting from any ideas, methods, instructions or products referred to in the content.